



## UWS Academic Portal

### Direct detection of delayed high energy electrons from the $^{181}\text{Ta}$ target irradiated by a moderate intensity femtosecond laser pulse

Savel'ev, A.; Chefonov, O.; Ovchinnikov, A.; Agranat, M.; Spohr, K M

*Published in:*  
Plasma Physics and Controlled Fusion

*DOI:*  
[10.1088/1361-6587/aa5427](https://doi.org/10.1088/1361-6587/aa5427)

Published: 30/01/2017

*Document Version*  
Peer reviewed version

[Link to publication on the UWS Academic Portal](#)

#### *Citation for published version (APA):*

Savel'ev, A., Chefonov, O., Ovchinnikov, A., Agranat, M., & Spohr, K. M. (2017). Direct detection of delayed high energy electrons from the  $^{181}\text{Ta}$  target irradiated by a moderate intensity femtosecond laser pulse. *Plasma Physics and Controlled Fusion*, 59(3), [035004]. <https://doi.org/10.1088/1361-6587/aa5427>

#### **General rights**

Copyright and moral rights for the publications made accessible in the UWS Academic Portal are retained by the authors and/or other copyright owners and it is a condition of accessing publications that users recognise and abide by the legal requirements associated with these rights.

#### **Take down policy**

If you believe that this document breaches copyright please contact [pure@uws.ac.uk](mailto:pure@uws.ac.uk) providing details, and we will remove access to the work immediately and investigate your claim.

# Direct detection of delayed high energy electrons from the $^{181}\text{Ta}$ target irradiated by a moderate intensity femtosecond laser pulse

A Savel'ev<sup>1,2,\*</sup>, O Chefonov<sup>1</sup>, A Ovchinnikov<sup>1</sup> and M Agranat<sup>1</sup>, K M Spohr<sup>3,4</sup>

<sup>1</sup> Joint Institute for High Temperatures of Russian Academy of Sciences, Izhorskaya st. 13, Bd. 2, Moscow 125412, Russia

<sup>2</sup> Physics Faculty and International Laser Center of M.V.Lomonosov Moscow State University, Leninskie gory, Moscow 119991, Russia

<sup>3</sup> School of Engineering & Computing, University of the West of Scotland, High Street, Paisley, PA1 2BE, Scotland, United Kingdom

<sup>4</sup> Scottish Universities Physics Alliance (SUPA), University of Glasgow, Kelvin Building, University Avenue, Glasgow, G12 8QQ, Scotland, United Kingdom

\* e-mail: [abst@physics.msu.ru](mailto:abst@physics.msu.ru)

**Abstract.** We depict an experimental study of delayed fast, negatively charged particles from femtosecond laser-plasma interaction at an intensity of  $I \sim 10^{17} \text{ Wcm}^{-2}$ . Plates of 2 mm thickness made of  $^{181}\text{Ta}$  (~100 % abundance) and natural W were used as targets. We distinguished certain delayed events due to detection of negative H<sup>-</sup>, C<sup>-</sup> and O<sup>-</sup> ions. However, most events which were delayed by 0.5  $\mu\text{s}$  – 5  $\mu\text{s}$  with respect to the instantaneous plasma formation caused by the laser pulses, were identified as electrons with energies of 3 keV -7 keV. A comparative analysis between the tantalum and tungsten spectra was undertaken. This revealed a close similarity between the measured spectrum for tantalum and the predicted spectrum for electrons arising from the internal conversion decay (IC) of the 6.237 keV nuclear isomeric state in  $^{181}\text{Ta}$ .

**Keywords:** femtosecond plasma, moderate intensity, isomeric nuclear levels, internal conversion

PACS: 23.20.Nx Internal conversion and extranuclear effects (including Auger electrons and internal bremsstrahlung), 52.70.Nc Particle measurements, 52.38.Ph X-ray,  $\gamma$ -ray, and particle generation ,29.30.Dn Electron spectroscopy

## 1. Introduction.

Plasma created by an intense femtosecond laser pulse, under its interaction with dense matter, has been studied for almost 25 years. Nowadays most attention is paid to relativistic  $I \approx 10^{18} \text{ Wcm}^{-2}$  or even ultra-relativistic intensities  $I > 10^{22} \text{ Wcm}^{-2}$ . However, lower, moderate, intensities are also important, especially as low intensity plasma can be routinely produced with commercially available lasers which have pulse energies of a few mJ, pulse durations in the order of 30-50 fs, and high repetition rates in the

Direct detection of delayed high energy electrons from the  $^{181}\text{Ta}$

kHz regime. These parameters provide for intensities up to  $I=10^{18}$   $\text{Wcm}^{-2}$ , inducing short lived, dense plasma which efficiently emits hard X-rays, accelerates multi-charged ions, *etc.* [1, 2].

The feasibility of low energy isomeric nuclear level excitation is an appealing, but still unanswered question in plasma physics. Different mechanisms for excitation were discussed and described from the first order processes, such as direct photoexcitation by plasma X-rays and electron inelastic scattering, to higher order processes such as Inverse Electronic Conversion (IEC) and others [3,4,5,6,7,8,9]. Femtosecond plasma created with a moderate intensity laser pulse is characterized by a high density of nuclei, a high peak flux of hard X-rays and energetic electrons. As such it is treated as the most appropriate plasma medium for an experimental search of low energy nuclear excitation [6,10].

A low energy nuclear excitation event can be detected through gamma decay yielding delayed X-ray photons, or an internal conversion (IC) process yielding delayed fast electrons. In plasma the IC process has specific features due to a deep ionization of atomic shells [11]. Two key experimental schemes are usually facilitated: (i) the direct nuclear excitation in plasma [12] and (ii) the nuclear excitation in a secondary target containing nuclei under study which are irradiated by X-rays and electrons from a primary laser plasma target [13]. The first scheme is characterized, generally, by higher excitation rates compared to the latter. The second scheme however allows studying a confined, tiny amount of a specific nuclei without the potential drawback that excited atoms may be sputtered from the target by the initial laser pulse. Moreover by using a secondary target, a higher signal-to-noise ratio can be achieved as the fast parasitic signals emerging from the direct flux of plasma X-rays and electrons can be suppressed. Both decay channels can be measured using these two schemes.

Experiments aimed at low energy isomeric level excitation report optimistic data [7, 12, 13, 14, 15] (except for [16]), but deduced nuclear excitation rates appear much larger than numerical estimates. That is why, until now, the feasibility of such a process in plasma has been considered as not confirmed. This situation stimulates interest for new experiments with a better signal-to-noise ratio, and the search for new possible mechanisms of low energy nuclear excitation with intense lasers.

In this paper, we present experimental data on detection of direct delayed electrons with energies of 3 keV -6 keV from the plasma created by a  $I\sim 10^{17}$   $\text{Wcm}^{-2}$  femtosecond laser pulse on the  $^{181}\text{Ta}$  target surface. It is shown that the spectrum of these electrons has a tight coincidence with the calculated spectrum of IC electrons associated with the decay of the isomeric 6.237 keV nuclear level in  $^{181}\text{Ta}$ . At first, we reason our choice of the target nuclei and present the expected spectrum for the IC electrons. After this the experimental setup is described. We present the experimental data on X-ray production from the Ta and W targets to confirm the similarities of the plasma created. This finding backs our experimental approach based on comparison of delayed fast electron spectra for these two targets. The last part of the paper is devoted to the measurement of the delayed electron spectra and its discussion.

## 2. Problem formulation.

Most suitable for a proof-of-principle experiment regarding the direct detection of delayed IC electrons is stable  $^{181}\text{Ta}$ , as this isotope has an isomeric nuclear level with an energy of 6.237 keV and a half-life of 6.05  $\mu\text{s}$ . The IC coefficient of the related decay is  $\alpha = 70.5$  [17]. For a variety of reasons this lifetime is somehow optimal for such an experiment. Firstly, its relative shortness provides for an efficient isomeric level population in a dense short lived plasma. In addition, the half-life is much longer than the plasma duration, thus allowing a detection of the delayed IC electrons against the background mainly created by the prompt plasma electrons. The low energy of this isomer enables such studies at moderate intensities of  $10^{16} \text{ Wcm}^{-2}$  -  $10^{17} \text{ Wcm}^{-2}$ , and, the characteristic energy of the related hot conversion electrons amounts to a few keV which is well above a low energy background [6]. Moreover, it is also favorable that the  $^{181}\text{Ta}$  isotope is de-facto the only stable Ta isotope as its abundance is 99.88% in a natural sample, so no intruding signals from other Ta isotopes need to be accounted for.

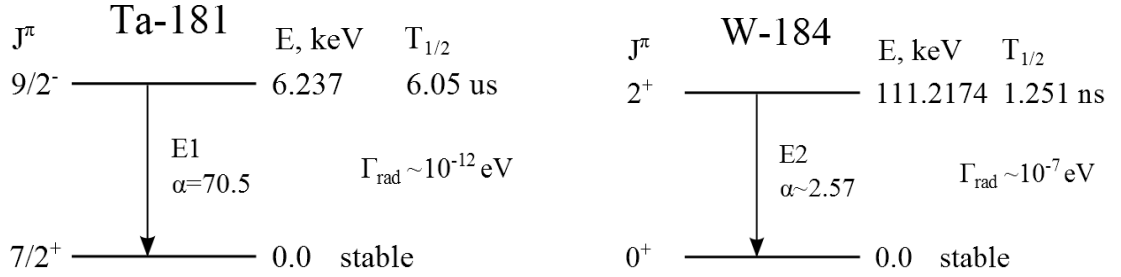


Figure 1. Energy level schemes for  $^{181}\text{Ta}$  (a) and  $^{184}\text{W}$  (b) isotopes.

Figure 1a presents the low energy level scheme of  $^{181}\text{Ta}$ . Figure 2 shows calculated probabilities of the IC process for different atomic shells of the Ta atom as well as the deduced spectrum of IC electrons. The expected energy spectrum of IC electrons is comprised mostly by the IC process through the  $M$ - and  $N$ -shells of the Ta atom. The most probable electron energies are 3.5 keV – 3.8 keV and 4 keV – 4.5 keV [18]. The IC process is followed by the  $MNN$ -Auger process, giving rise to delayed Auger electrons with energies below 2.7 keV. Hence an experiment should be aimed at the detection of electrons delayed by 0.5  $\mu\text{s}$  - 10  $\mu\text{s}$  with respect to the initial plasma formation which is assumed to be instantly. The energy range of 3.5 keV-7 keV should be surveyed.

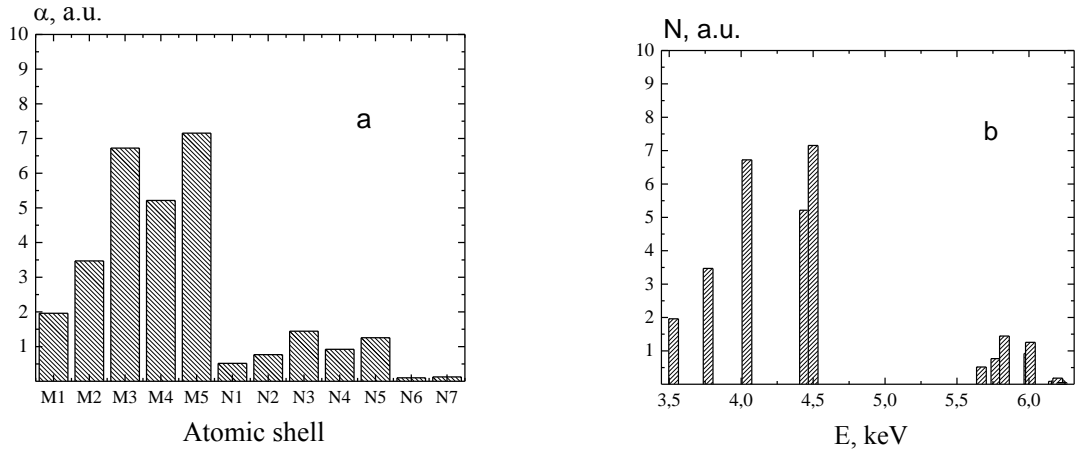


Figure 2 Partial probabilities  $\alpha$  of the IC process through different atomic shells (a) and an expected energy spectrum of IC electrons emerging from the isomeric level in  $^{181}\text{Ta}$  [18].

A tungsten target is used as a reference to estimate the influence of noise electrons. Tungsten consists of four stable isotopes,  $^{182}\text{W}$ ,  $^{183}\text{W}$ ,  $^{184}\text{W}$  and  $^{186}\text{W}$  with different abundances (see Table 1) all of which have almost the same atomic shell structure and atomic mass as  $^{181}\text{Ta}$ . This allows to presume that very similar plasma characteristics will apply in tungsten as in tantalum (see also experimental data below). Moreover, the first excited nuclear states of these isotopes are quite high in energy (see Table 1 and sample data for the  $^{184}\text{W}$  isotope in Figure 1b); thus the probabilities for a population of all these W levels at moderate laser intensities are negligibly low.

**Table 1.** Specific properties of the first excited nuclear states of stable W isotopes.

W isotope atomic weight	Natural abundance, %	Level energy, keV	Lifetime, ns	Polarity	$\alpha$
182	26	100.1	1.38	E2	3.89
183	14	46.48	0.188	M1+E2	8.63
		99.07	0.77	E2	4.12
184	30	111.2	1.25	E2	2.57
186	28	122.62	1.0	E2	1.81

### 3. Experimental setup

Experimental scheme is shown in Figure 3. It is similar to the scheme used previously [14], except for the lack of a secondary target and the electron spectrometer placing. We used femtosecond laser pulses from the Ti:Sa laser with a central wavelength of 795 nm, energy of 1.5 mJ, duration of 40 fs and repetition rate of 1 kHz. This laser system is a part of the unique scientific facility ‘‘Terawatt femtosecond laser complex’’ at the Joint Institute for High Temperatures of the Russian Academy of Sciences. The off-axis parabolic mirror (OAP, 2’’ in diameter, 3’’ focal length, 97% reflectivity) focused this radiation onto a flat target plate at  $45^\circ$  inclination. The on-target intensity amounted to  $I \sim 10^{17} \text{ Wcm}^{-2}$  with the focal spot diameter being  $\sim 5.5 \mu\text{m}$  (FWHM). An instantaneously moving Lavsan film with a

thickness of 20  $\mu\text{m}$  prevented the sputtering of plasma debris onto the parabolic mirror. The polished Ta and W target plates had a thickness of 2 mm lateral dimensions of 25 mm x 25 mm. The plates were mounted on a 5-axis motorized optical stage system which allowed a steering of three linear and two angular axes. An optical visualization system checked the focusing quality of the laser beam. During experiments the target was translated with a linear speed of 5  $\text{mm}\cdot\text{s}^{-1}$  in the plane perpendicular to the laser beam axis. The vacuum in the interaction chamber was held at  $\sim 10^{-8}$  atm.

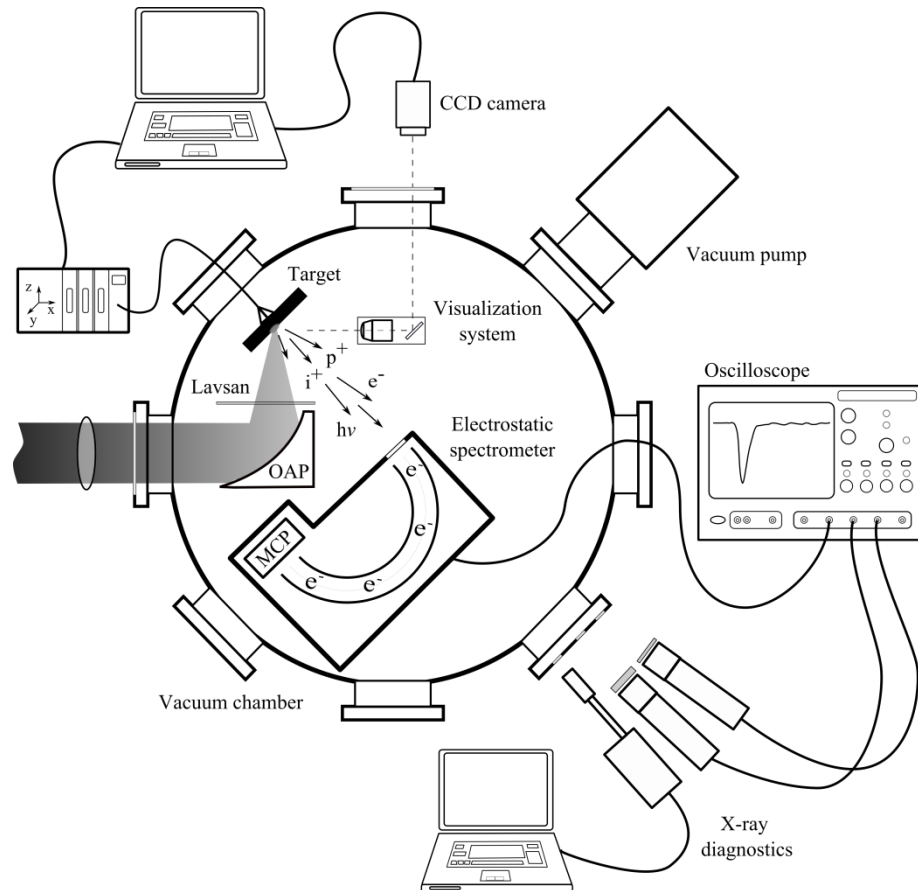


Figure 3. Schematics of the experimental setup.

We used scintillation detectors (NaI(Tl) 25 mm thick coupled with PMT) and an Amptek XR-100T-Cd spectrometer to assess plasma X-ray radiation. The latter was used to measure X-ray spectra in a single quantum counting regime [19], so it was placed outside the vacuum chamber in air, 90 cm apart from the target and with a 400  $\mu\text{m}$  aperture x-ray collimator in front of it. Spectra were measured over 30 s (30,000 laser shots at 1 kHz). The electrostatic spectrometer was a semi-cylindrical analyzer with a spectral energy resolution of 10% equipped with a chevron Micro Channel Plate (MCP), which is described elsewhere in detail [20]. The spectrometer was used for energy and time-of-flight resolved

measurements of the ion and electrons particles which were emitted from the plasma. The spectrometer was placed in a special metallic grounded shield made from copper and lead to eliminate electronic noise. Moreover this grounding suppressed other induced intruding signals resulting *e.g.* from the plasma generated RF electromagnetic waves, X-rays or fast electrons. All cables which connected the spectrometer to the vacuum flange were also carefully shielded and grounded. We changed the deflecting voltage of the cylindrical analyzer to measure electron energy spectra within a 3 keV -15 keV range. The shielded spectrometer was placed 25 cm apart from the target along a normal to its surface. The solid angle of the input window of the spectrometer was determined by the input led aperture with a 2 mm in diameter and accounts to  $\Omega \sim 6 \times 10^{-5}$  sr. The digital multichannel oscilloscope Tektronix TDS7054 was used for the data acquisition from the spectrometer and the scintillation detectors. The temporal resolution of the spectrometer together with its acquisition system was only  $\sim 1$  ns, thus well suited for decay studies in the  $\mu\text{s}$  regime.

#### 4. Experimental results

The comparative plasma X-ray study of W and Ta targets was the principal part of our experiment. We measured total X-ray yield and X-ray spectra for both targets and confirmed that the plasma conditions were almost equal in terms of X-ray flux and spectrum. It is worth noting that the partial overlapping of interaction areas occurred for consecutive laser shots at the repetition rate of laser pulses  $\sim 1$  kHz and translation speed of  $v=5$  mm.s $^{-1}$ . This resulted in a groove pattern formation in the irradiated target surface, and even in the X-ray yield enhancement [21,22]. We checked this effect by changing the translation speed  $v$  of the target. The optimum speed was determined to be  $v = 5$  mm.s $^{-1}$  as at this velocity the X-ray yield achieved maximal values. At this speed approximately 2-3 consecutive laser shots impinge almost within the same area on the target surface. Figure 4 shows that X-ray spectra of the Ta and W targets. Both spectra have the same slope especially visible at the high energy tail. Also, the Ta and W X-ray spectra show the same amplitude. The only slight differences, as expected, are the spectral positions of the associated X-ray lines which are due to the tiny differences in the binding energies of L shell electrons for Ta and W.

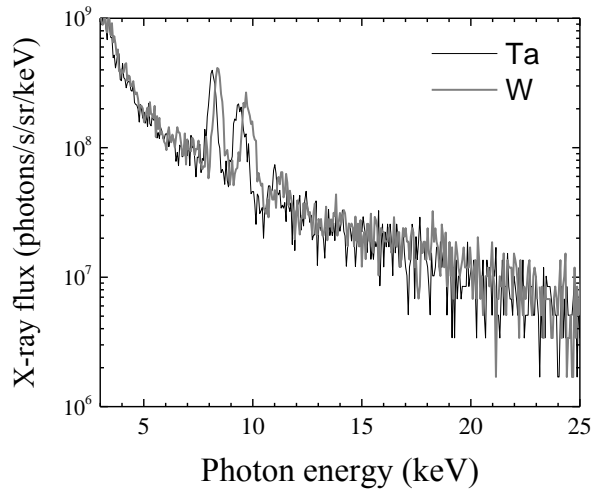


Figure 4. X-ray spectra for Ta and W targets obtained at a translation speed of  $v = 5 \text{ mm}\cdot\text{s}^{-1}$ .

The electrostatic spectrometer measured the flux of charged particles from the plasma. The deflection voltage applied to the semi-cylindrical analyzer allowed to determine the energy  $E_j$  per the elementary charge and the charge sign of a detected particle. The measurement of the particles time-of-flight was undertaken. An energy range between  $E_j = 3\text{-}7 \text{ keV}$  was surveyed. Each  $E_j$  value comprised 8000 independent laser shots. A typical single shot record is shown in Figure 5 for  $E_j = 4.5 \text{ keV}$ . The huge, noisy spike at zero time is due to detection of direct plasma emission such as X-rays and fast electrons, while fast negative short pulses at  $0.669 \mu\text{s}$  and  $2.761 \mu\text{s}$  were caused by single negatively charged particles.

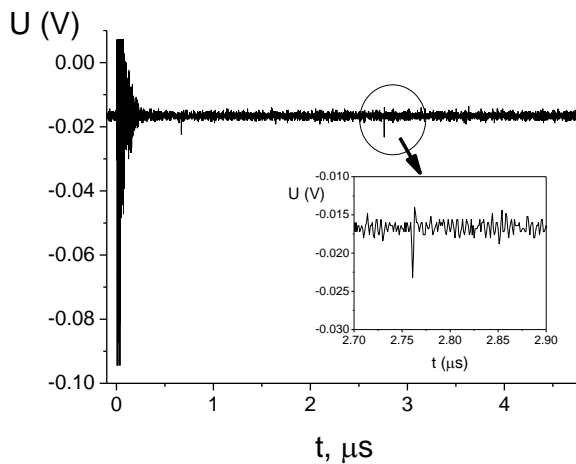


Figure 5. A sample single shot record obtained with the Ta target for a particle energy of  $4.5 \text{ keV}$ . The inset magnifies the single particle event which appeared  $2.761 \mu\text{s}$  after the initial laser pulse.



Further analysis of the data was done between 0.2  $\mu\text{s}$  to 4.5  $\mu\text{s}$ . The lower time limit was restricted by the huge direct plasma emission signal after the laser pulse, while the sample length of the Tektronix TDS7054 determined the maximum surveying time.

To obtain energy spectra of delayed particles as well as temporal envelopes at all energies  $E_j$  the whole time interval was divided in time-bins of a length of 0.5  $\mu\text{s}$ . Single spikes in each recorded spectra were counted for each energy  $E_j$ . These yielded a number of events  $N_{ij}$  at the given energy  $E_j$  within the time bin interval of  $\Delta t_i$ . This procedure was applied for the Ta as well as for the W measurement.

Surprisingly, all the dependencies  $N_{ij}(\Delta t_i)$  showed non-monotonic behavior with two maxima, those positions changed from 2.5 to 0.8  $\mu\text{s}$  with  $E_j$  increasing from 3 keV to 7 keV. Knowing flight-path for these particles, their energy per charge and charge sign, we confirmed that these were negative ions of hydrogen ( $\text{H}^-$ ) and oxygen ( $\text{O}^-$ ). Negative ion production from a femtosecond plasma was first observed and explained in [23].

Hence, we excluded events observed at time intervals corresponding to such ions' arrival at the detector from further analysis. An interval center was calculated as time-of-flight of a specific negative ion at a given energy  $E_j$ , while its width – from the spectrometer energy resolution (the full width changed from 0.1  $\mu\text{s}$  to 0.35  $\mu\text{s}$  depending on the energy  $E_j$ ). The data obtained after the exclusion procedure lost temporal dependence – the number of events  $N_{ij}$  did not depend on time for all energies  $E_j$ , at least within the limits of the statistical error. This was due to the arbitrary short detection interval of 3.5  $\mu\text{s}$  which is substantial shorter than the to the half-life of the  $^{181}\text{Ta}$  isomeric nuclear level ( $\sim 6 \mu\text{s}$ ).

Figure 6a presents spectra of delayed events which were summed over the full detection time at a given energy  $E_j$  as described. Since the ejection of IC electrons as well as Auger processes are both quite fast processes that happen within the  $\mu\text{s}$  time scale, we do expect that the spectrum observed within a 3.5  $\mu\text{s}$  interval is the same as the spectrum integrated over a few lifetimes of the  $^{181}\text{Ta}$  isomeric nuclear level. We split all the 8000 runs at a given energy in 16 groups, 500 runs each, and calculated the number of events in each group, with the mean value for 16 groups and its standard deviation  $\sigma$ . Each data point in Figure 6a corresponds to the mean value and  $\sigma$  divided by the factor of 500 for normalisation. The spectrum in Figure 6b presents the difference between the Ta and W spectra. There are two spectra intervals where the number of events for the  $^{181}\text{Ta}$  target is reliably higher than that for the W. This intervals are between 3.5 keV - 4.7 keV and 5.7 keV - 6.2 keV.

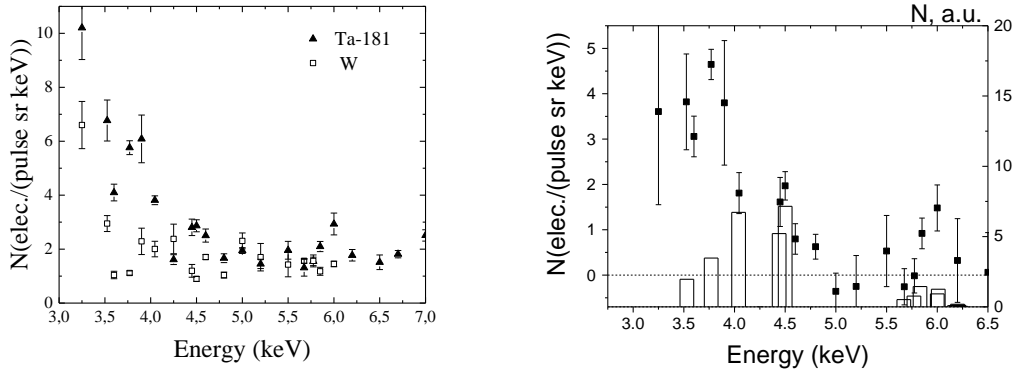


Figure 6. Spectra of delayed electrons from the Ta and W targets (a) and difference between these two spectra (b). In Figure 6b the calculated spectrum of IC electrons from the 6.237 keV isomeric level of  $^{181}\text{Ta}$  isotope is also shown by the open bars.

## 5. Discussion & conclusions

Figure 6b also contains the calculated spectrum of delayed electrons from IC of the 6.237 keV isomeric level of the  $^{181}\text{Ta}$  isotope. Note that the latter spectrum corresponds to the IC decay in a fully dressed Ta atom. Impact ionization in plasma almost certainly will influence the theoretical spectrum, especially if one accounts for the IC probabilities from the upper atomic shells [11]. It can be clearly seen from Figure 6b that for both intervals, 3.5 keV-4.7 keV and 5.7 keV - 6.2 keV, the differential spectrum has amplitudes well above zero. This, in turn could be linked to a group of certain IC processes from the Ta isomeric level. The prominent increase in the number of delayed electrons at energies  $E_j < 4$  keV should be attributed to the secondary Auger process following the IC decay [13]. The number of excited Ta nuclei in a single shot can be estimated from the experimental data in Figure 6b at IC electron energies of around 4.5 keV and 5.9 keV. This yields  $30 \pm 10$  and  $50 \pm 15$  nuclei per shot, respectively. Assuming that the excitation volume is  $7 \times 7 \times 2 \mu\text{m}^3$  and the absorption length of a 6 keV photon is  $\sim 2 \mu\text{m}$ , the excitation efficiency amounts to  $\sim 10^{-11}$ . Certainly this estimate is very rough and does not take into account plasma expansion, finite length of an IC electron free path in plasma, *etc.*

Still, this value is of such a high order of magnitude that it cannot be explained from the simple photoexcitation process by plasma x-rays or inelastic scattering by plasma electrons [9] and based on our current understanding, two possible scenarios may apply. Firstly, those peaks in the energy spectrum of delayed events are due to some specific process in atomic shells of a Ta atom, or, secondly, the isomeric nuclear level excitation in our experimental conditions passes through a different, yet still unclear channel that certainly depends on an atomic shell structure. Joint efforts of theoreticians and experimentalists are needed to address these issues. Novel approaches for isomeric nuclear excitation in plasma, and more precise experiments with better yields leading to an enhancement of the statistical significance are demanded.

## 6. Acknowledgements

The experimental part of this work has been carried out at Joint Institute for High Temperatures of the Russian Academy of Sciences (JIHT RAS) and was supported by the Russian Science Foundation (grant #14-50-00124).

## 7. References

- 
- [1] Gibbon P, Forster R 1996 Short-pulse laser - plasma interactions *Plasma Phys. Controlled Fusion* **38** 769-793
- [2] Ivanov K A, Uryupina D S, Volkov R V, Shkurinov A P, Ozheredov I A, Paskhalov A A, Eremin N V, Savel'ev A B 2011 High repetition rate laser-driven  $K\alpha$  X-ray source utilizing melted metal target *Nuclear Instruments and Methods in Physics Research A* **653** 58–61
- [3] Letokhov V S, Yukov E A 1994 Excitation of isomeric low-lying levels of heavy nuclei in a laser-produced plasma *Laser Physics* **4** 382-387
- [4] Gol'danski V I, Namiot V A 1976 Excitation of isomeric nuclear levels by laser radiation via the mechanism of inverse internal electron conversion *JETP Lett.* **23** 451
- [5] Arutyunyan R V *et al* 1991 Excitation cross-section for  $^{235}\text{U}$  isomer in plasma created by beam of electrons *Sov.J.Nucl. Phys.* **53** 23
- [6] Harston M R, Chemin J F 1999 Mechanisms of nuclear excitation in plasmas *Phys. Rev. C* **59** 2462
- [7] Andreev A V *et al* 2000 Excitation and decay of low-lying nuclear states in a dense plasma produced by a subpicosecond laser pulse *JETP* **91** 1163–1175
- [8] Gobet F *et al* 2011 Nuclear physics studies using high energy lasers *Nucl.Instrum.Methods Phys. Res.A* **653** 80–3
- [9] Tkalya E V 1991 Theoretical interpretation of experimental results on excitation of the isomer  $^{235}\text{U}$  (76.8 eV) in a plasma *JETP Lett.* **53**, 463,  
Tkalya E V 004 Mechanisms for the excitation of atomic nuclei in hot dense plasma *Laser Phys.* **14** 360–77
- [10] Andreev A V *et al* 1997 Nuclear excitation in hot dense plasma: feasibility of experimental study with  $^{201}\text{Hg}$  *JETP Lett.* **66**, 331
- [11] Andreev A V, Gordienko V M, Savel'ev A B, Tkalya E V, Chutko O V 2001 On the possibility of controlling the decay rate of low-lying nuclear levels upon excitation in a laser plasma *Quantum Electronics* **31** 567 – 568  
Andreev A V, Gordienko V M, Savel'ev A B, Tkalya E V, Chutko O V 2003 Decay of low-energy nuclear levels in femtosecond laser plasma: The effect of the charge state on the probability of decay via internal electron conversion *Laser Physics* **13** 1–6
- [12] Andreev A V *et al* 1999 Excitation of tantalum-181 nuclei in a high-temperature femtosecond laser plasma *JETP Lett.* **69** 371–6
- [13] Golovin G V, Savel'ev A B, Uryupina D S, Volkov R V 2011 Internal electron conversion of the isomeric Fe-57 nucleus state with an energy of 14.4 keV excited by the radiation of the plasma of a high-power femtosecond laser pulse *Quantum Electron.* **41** 222–6
- [14] Chefonov O V, Ovchinnikov A V, Yurkevich A A, Romashevskiy S A, Shulyapov S A, Petrovskiy V P, Savel'ev A B, Agranat M B 2014 Experimental search for low energy nuclear excitation by femtosecond plasma *Laser Phys.* **24** 116002
- [15] Afonin V, Kakshin A, Mazunin A 2010 Experimental study of the excitation of rhodium isomer in a plasma produced by a picosecond laser pulse *Plasma Phys. Rep.* **36** 250–5  
Afonin V, Kakshin A, Mazunin A 2011 Excitation of the isomeric states of silver isotope nuclei in the plasma produced by a subrelativistic picosecond laser pulse *Plasma Phys. Rep.* **37** 615–20
- [16] Gobet F *et al* 2008 Particle characterization for the evaluation of the  $^{181\text{m}}\text{Ta}$  excitation yield in millijoule laser induced plasmas *J. Phys. B: At. Mol. Opt. Phys.* **41** 145701
- [17] *Nuclear Data Sheets*, Ed. by M J Martin (Academic, New York, 1966–1986), Vol. **46**
- [18] Kibedi T, Burrows T W, Trzhaskovskaya M B, Davidson P M, Nestor Jr C W 2008 Evaluation of theoretical conversion coefficients using BrIcc *Nucl. Instr. and Meth. A* **589** 202–229
- [19] Fourment C *et al* 2009 Broadband, high dynamics and high resolution charge coupled device based spectrometer in dynamic mode for multi-keV repetitive x-ray sources *Rev. Sci. Instrum.* **80** 083505
- [20] Gordienko V M, Lachko I M, Mikheev P M, Savel'ev A B, Uryupina D S, Volkov R V 2002 Experimental characterization of hot electron production under femtosecond laser plasma interaction at moderate intensities *Plasma Phys. Control. Fusion* **44** 2555–68
- [21] Vorobyev A, Guo C 2005 Enhanced absorptance of gold following multipulse femtosecond laser ablation *Phys. Rev. B* **72** 195422

- [22] Gavrilov S A, Golishnikov D M, Gordienko V M, Savel'ev A B, Volkov R V 2004 Efficient hard x-ray source using femtosecond plasma at solid targets with a modified surface *Laser and Particle Beams* **22** 301-306
- [23] Volkov R. V, Gordienko V M, Lachko I M, Mikheev P M, Mar'in B V, Savel'ev A B, Chutko O V 2002 Generation of high-energy negative hydrogen ions upon the interaction of superintense femtosecond laser radiation with a solid target *JETP Letters* **76** 139–142
- Chutko O V, Gordienko V M, Lachko I M, Mar'in B V, Savel'ev A B, Volkov R V 2003 High-energy negative ions from expansion of high-temperature femtosecond laser plasma *Applied Physics B* **77** 831-837